Journal of Basrah Researches (Sciences) **50**(1), 1 (2024)
DOI: https://doi.org/10.56714/bjrs.50.1.1

QSPR study to predict the detonation velocity of explosives with emphasis on studying the electronic spectra of RDX

Thaer Majid Hamid*, B.A. Saeed

Department of chemistry, College of Education for pure sciences, University of Basrah, Basrah, Iraq.

ARTICLE INFO

Received 09 March 2023
Accepted 28 March 2023
Published 30 June 2024

Keywords:

QSPR, Descriptors, AIM, of RDX.

Citation: T. M. Hamid, B.A. Saeed, J. Basrah Res. (Sci.) **50**(1), 1 (2024).
DOI:https://doi.org/10.56714/bjrs.50.1.1

ABSTRACT

The study devoted to calculate and interpret the electronic spectra of the RDX molecule. The six isomers of the RDX molecule were geometry optimized with the MP2/cc-pVTZ level of theory. The twist isomer was shown to be the most stable isomer. The electronic spectra of the six isomers were calculated with acetonitrile as a solvent. The electronic spectra were calculated using the PBE0/def2-tzvppd level of theory in acetonitrile as a solvent. The combined PBE0/def2-tzvppd// MP2/cc-pVTZ methods succeeded in reproduce fairly the experimentally measured main band at 236 nm. The calculated wavelength was 237 nm and the band was shown as mainly originated from the HOMO to LUMO transition with a transition probability of 0.49688 which is 49.4% of the overall transitions responsible for this band. The calculated spectrum of the most stable isomer (twist) was most relevant to the experimental spectrum. In order to predict the detonation velocity of explosives the Quantity Structural-Property Relationship calculations were done and a statistical empirical equation was built based on the measured detonation velocity of well-known explosives and several structural and electronic descriptors.

1. Introduction

RDX (Research Department Explosive) or cyclotrimethylene-trinitramine is a well-known energetic explosive and monopropellant [1-7]. It is characterized by high detonation power and low sensitivity. The later property makes it very suitable for storage and mostly used in explosive mixture in order to reduce their sensitivity for shock and heat. It is characterized by six isomeric conformers stemmed from the orientation of its three nitro groups with respects to the molecule ring. The nitro groups could have the all-equatorial spatial configuration which in this case referred to as AAA or all axial configuration which is referred to as EEE, or have a variety of formations of these orientations. The central ring of the molecule could have the both the chair and boat forms as well the twisted form. Many crystallographic and computational articles dealing with its structural, electronic, spectral, and thermal decomposition properties were published. Crystallographic studies showed that it has five polymorphic forms alpha, eta, gamma, eta and sigma with first is the stable form at ambient pressure and temperature. In RDX the ring is puckered and one of the N-NO2 groups is co-planar which the

*Corresponding author email: Thiaer270@gmail.com

ISSN: 1817-2695 (Print); 2411-524X (Online)
Online at: https:// jou.jobrs.edu.iq

others are slightly bent. Concerning the geometry of RDX conformers several theoretical studies were done using B3LYP, MP2, and CCSD(T) methods[8, 9] . The results are in general with the AAA and twist conformers as the most stable structures. The electronic spectrum of RDX in acetonitrile was studied by Cooper et al. [10] and the used functionals and basis sets failed to reproduce the maximum wavelength of the main absorption which appears at 236 nm, and the predicted one was 225 nm. No systematic study was done previously to build empirical equations for the calculation of the detonation of the explosives. This work is devoted to investigate the relative stability and the electronic spectra as well as build a model empirical equation for the prediction of the detonation velocity of explosives.

2. Computational methods

All the calculations were done with the Gaussian 16 software [11, 12]. The electronic structures of the studied molecules were sketched with Gaussview program and freely geometry optimized in the gas phase using the MP2/cc-pVTZ level of theory. The stability of the structure was demonstrated by calculating the vibrational spectra at the same level of theory. All the calculated vibrational spectra showed no imaginary frequencies indicating that all the structures are global minima at the potential energy surface. The electronic spectra were calculated using the PBE0/def2-tzvppd level of theory in acetonitrile as a solvent. The notations AAA, AAE, EEE and EEA are stands for axial-axial-axial, axial-axial-equatorial, equatorial-equatorial-equatorial and equatorial-equatorial-axial defining the orientations of the nitro groups with respect to the molecule ring. The descriptors that are used for building the model empirical equation was calculated using the program Materials Studio while atom-in-molecules (AIM) values were calculated using the AIMAll program. The experimental detonation values were gathered from variety of scientific papers.

3. Results and discussion

3.1. The relative stability of the RDX isomers

The electronic structures of the possible isomers of RDX are shown in figure 1. The isomers stem their structural differences mainly from the geometrical structure of the central ring of the molecules which in turn lead to different spatial arrangements of the three nitro groups within the molecule.

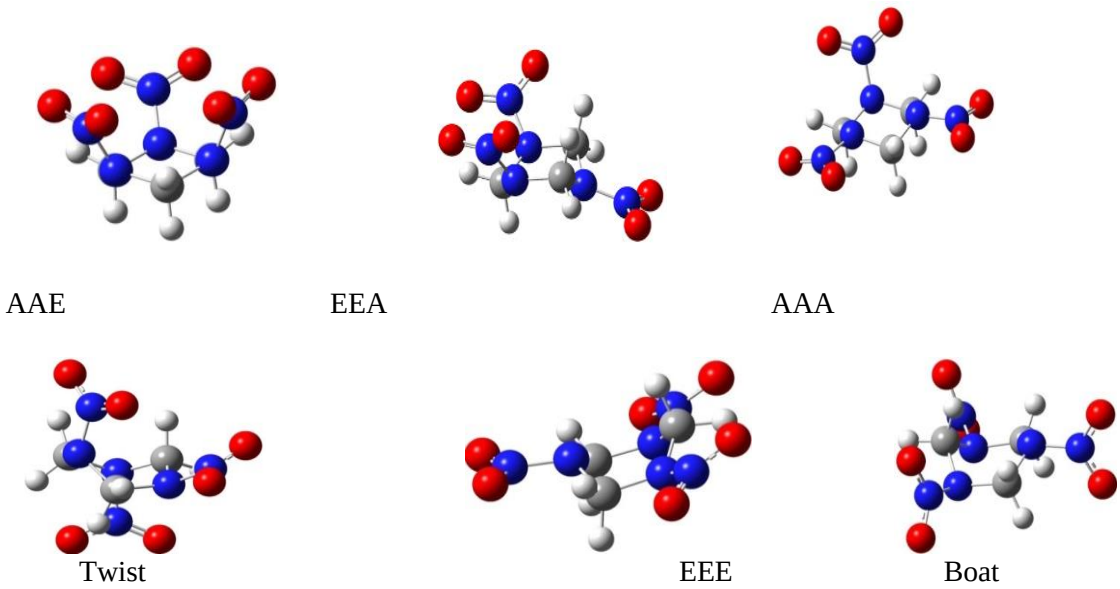

Fig.1. The electronic structures of the possible isomers of RDX as calculated at the MP2/cc-pVTZ level of theory.

Table 1 contains some of the electronic and structural properties of the studied isomers calculated at the MP2/cc-pVTZ level of theory. From table 1 it is shown that the stability of the isomers is in

the sequence twist > AAA> AAE > EEE > EEA > boat with relative energies of 0, 4.20, 5.25, 5.25, 30.72 and 73.25 kJ mol-1 respectively. Accordingly the most stable isomer is the twisted isomer. This could be rationalized as in this isomer the spatial directions of the nitro groups make the less sterically crowded configuration.

Table 1. Total energies (hartee), relative energies (kJ mol-1) and some structural properties (Å) of the isomers of RDX calculated at the MP2/cc-pVTZ level of theory.

NO	Isomer	Total Energy hartree	ΔE (H)	(N–O) Å	(N–N) Å	(C–N) Å	(C–H)Å
1	(AAA)	-896.00045	0.0019	1.2032	1.4026	1.4530	1.0815
2	(AAE)	-895.991337	0.0110	1.2030	1.4091	1.4442	1.0825
3	(EEA)	-895.999555	0.0028	1.2054	1.3881	1.4554	1.0845
4	(EEE)	-895.973470	0.0289	1.2030	1.3778	1.4444	1.0825
5	(boat)	-895.122937	0.8794	1.2034	1.4508	1.4659	1.0931
6	(twist)	-896.002410	0.0000	1.2063	1.4050	1.4633	1.0834

Table 1, as well shows that within the structural properties the N-O bond length in the twist isomer has the highest value with a length of 1.2063 Å which make this bond the most liable to break in comparison with the other isomers.

3.2. The calculated electronic spectra of the RDX isomers.

The experimental electronic structure of RDX in acetonitrile is characterized by the presence of two bands, the shortest at 196 nm while the other appears as a shoulder at 336 nm. Several studies were undertaken to predict the spectrum of RDX at different levels of theory, the most comprehensive is that of Copper et al [13, 14] which based on the electronic structure that was calculated by the level B3LYP/6-311+G(d,p). The electronic spectra were calculated at several functional which included B3LYP, CAM-B3LYP, wB97XD and PBE0 assisted with the basis set 6-311+G(d,p) but all the methods failed to reproduce the experimental wavelengths and estimated a values of the long wavelength band at 225 nm against 236 nm for the experimentally measured one. For the correct interpretation of the origins of these bands, a fair correct theoretical prediction of the band positions is needed. This is may be due to the problematic B3LYP functional [15] which has many shortages, one of them is its failure to calculate the charge dispersion in the molecules which could be arises from the resonance in the nitro groups which leads to delocalization of the charge density. In this study the MP2 method [16] which take into account this matter in conjunction with the cc-pVTZ basis set is used for the geometry optimization of the structures. On the other hand the PBE0/def2—tzvppd level of theory was used to calculate the electronic spectra. The calculated electronic spectra of the six isomers of the RDX are gathered in Figure 2 and the calculated bands are shown in Table 2.

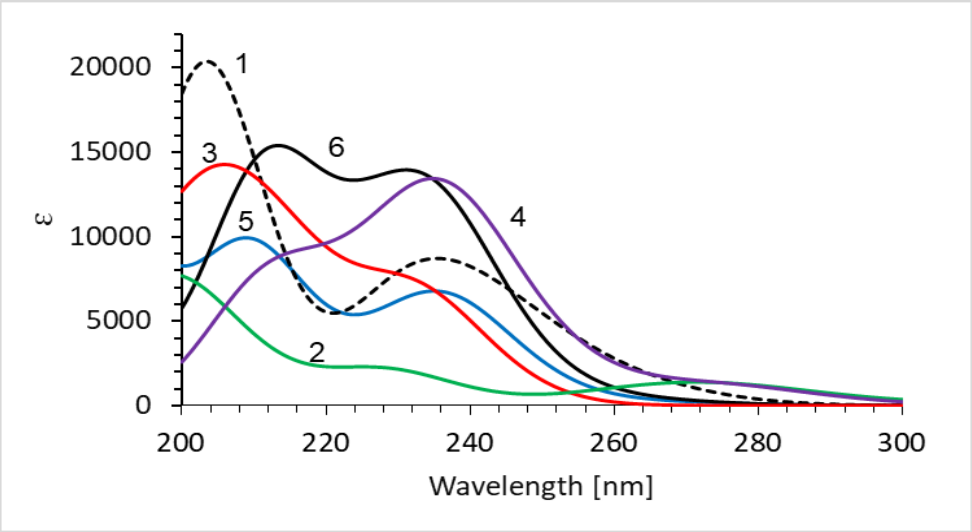

Fig.2. The calculated electronic spectra of the six isomers of the RDX in acetonitrile at the level PBE0/def2-tzvppd. 1) boat , 2)eee , 3) eea , 4) aae , 5) aaa , 6) twist .

Table 2. The calculated electronic bands (nm) of the six isomers of the RDX at the level PBE0/def2-tzvppd in acetonitrile.

Isomer	Band I	Band II	Other bands
aaa	235.0	211.6	---
aae	236.5	212.5	---
Boat	231.4	206.5	261.4, 245.0
eea	232.7	200.0	---
eee	227.5	198.7	352.8, 277.0
twist	237.0	208.0	---

It could be seen from Figure 3 that the electronic spectrum of the twist isomer is the most relevant to the experimental spectrum [17]. This is also shown in Table 2 where the calculated spectrum contains two bands at 237 and 208 nm. Accordingly, the calculated spectrum of this isomer was taken is a representative for the experimental electronic spectrum of the RDX. The long band is in fair agreement with the 236 nm experimental band. This gives evidence that the twist isomer is the most stable isomer. Figure 3 and Table 2 show as well, that the calculated spectra for other isomers are within the range 227-236 nm in addition to other bands at 261, 245, and 353, 277 nm in the isomers boat and EEE respectively. To interpret the bands origin of the electronic spectrum the bands and the corresponding transitions are gathered in Table 3.

Table 3. The bands and corresponding transitions of the electronic spectrum of the isomer twist.

Band	Transition	Transition Probability	Oscillator strength
237	57 → 58	0.49688	0.1339
	47 → 59	0.17940	
	56 → 58	0.27227	
	56 → 59	0.26305	
208	47 → 58	0.11239	0.1995
	54 → 60	0.10584	
	57 → 60	0.64966	

As could be seen from Table 3 the band at 237 nm arises from four transitions. The most significant transition arises from the HOMO (57) to the LUMO (58) with a transition probability of

0.49688 which is 49.4% of the overall transitions. The band at 208 nm mainly originated from the transition from HOMO to LUMO+2 with a transition probability of 0.64966 representing 84.4% within the overall transitions that are responsible for this band. The oscillator strength can be a measure for the band intensity, and the oscillator strengths of the predicted bands are also shown in Table 3. The oscillator strengths of the bands 237 and 208 are 0.1339 and 0.1995 respectively shong a higher intensity of the later which is in accordance with the experimental spectrum [18, 19].

In addition, to shed more light on the electronic transitions the hole-electron proedure could be used to track the transition of the electronic density accompanied the spectra. This is represented in figures 4 and 5.

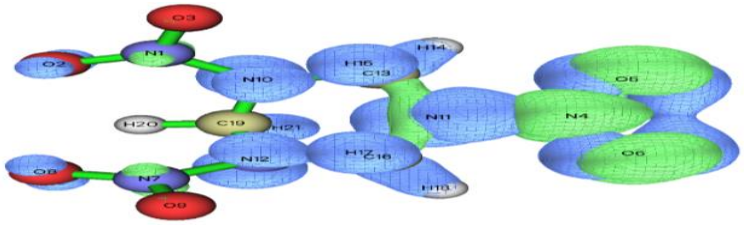

Fig.3. The main hole (blue) and electron (green) distribution regions of the transition are responsible for the band 237 nm.

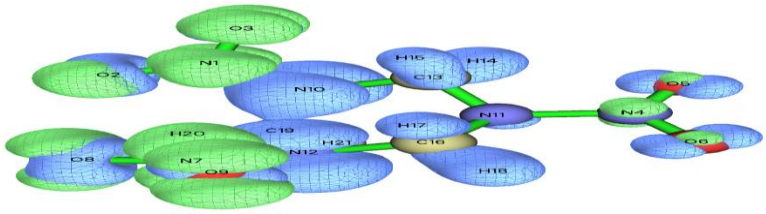

Fig.4. The main hole (blue) and electron (green) distribution regions of the transition are responsible for the band 208 nm.

From Figure. 4 it could be seen that for the band 237 nm, the hole is mainly separated over the nitrogen atoms especially nitrogen-4 as well as oxygen-5 and oxygen-6, while the electron is mainly separated over the nitrogen-4, oxygen-,5, and oxygen-6 respectively. This means that the electronic transition responsible for this band is $\pi \leftarrow \pi^*$ kind and the electronic density is transferred mainly within the amino group. In the same direction, the transition for band 208 could be disused. It is obvious from figure 5 that the donor regions are centered over nitrogen-10 and nitrogen-12 atoms within the molecule ring (sigma electrons and n nonbonded pair of electrons could be a source as well) and the oxygen atoms 2 and 8. The acceptor regions are sseparatedover π electrons in the amino group mainly which leads to the conclusion that this band arises from a complicated of transitions like $n \rightarrow \pi^*$ and $\sigma \rightarrow \pi^*$. This is further supported by the Natural Orbital Transitions (NOT) calculations shown in Figures 6 and 7.

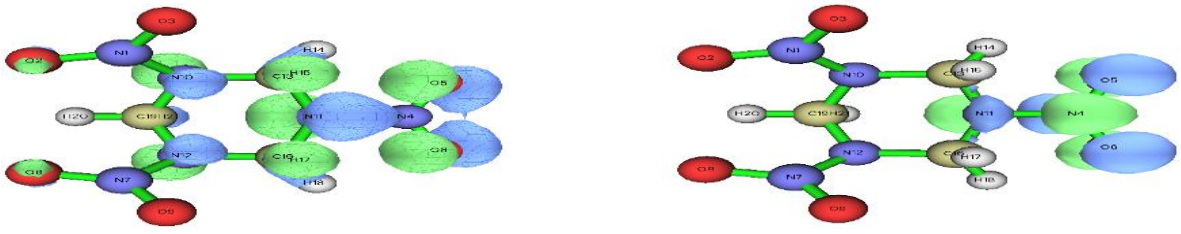

The donor orbital The acceptor orbital

Fig.5. The natural orbital transitions responsible for the band 237 nm.

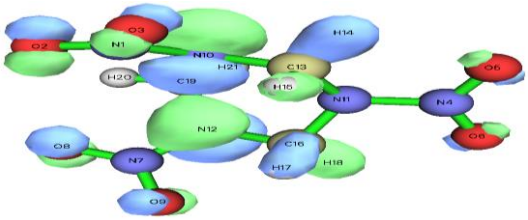

Fig.6. The donor orbital

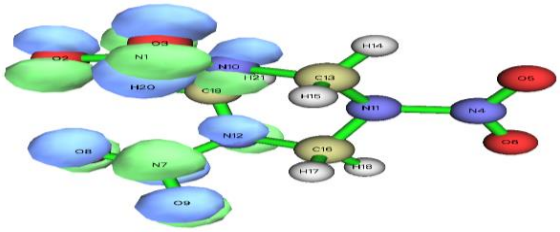

Fig.7. The acceptor orbital

According to figures 5 and 6 which show the natural orbital transitions for the bands 237 and 208 nm respectively, the electronic charge of the donor orbital in the band 237 nm is centered on the nitrogen-11 and the two oxygens while it is separated over the π electrons of the nitro group in the case of the acceptor orbital. On the other side concerning the band 20 nm the charge density is localized over the nitrogen atoms in the ring as an acceptor while it is over the π system in the amino groups as a donor.

3.3. Quantitative Structure-property Relationship study

The study is also devoted to building an empirical model serve to predict the detonation velocity of the explosives. A trial group of 27 well-known explosives was chosen for this study and are shown in Table 4. The descriptors used for the building of the empirical equation are gathered in Table 5.

Table 4. The explosive that are used as the trial group in this study.

N0.	Explosive	Detonation velocity	Reference
1	(HMX) 1,3,5,7-tetranitro-1,3,5,7-tetrazocane	9320	[20]
2	(3at) 6-azido-8-nitrotetrazolo[1,5-b]pyridazin-7-amine	8746	[21]
3	(RDX) 1,3,5-trinitro-1,3,5-triazinane	8795	[22]
4	Picric acid	7376	[44, 45]
5	(ETN) Erythritol tetranitrate	8015	[23]
6	(FOX-7) 2,2-dinitroethene-1,1-diamine	8870	[24]
7	(TNT) 2-methyl-1,3,5-trinitrobenzene	6959	[25]
8	(PETN) Pentaerythritol tetranitrate	8564	[26]
9	(TATB) Trinitrobenzene-1,3,5-triamine	8114	[27]
10	(TMETN) Trimethylolethane trinitrate	7050	[28]
11	Di-3,4(nitramino)furazan	9849	[29]
12	5-nitro-2H-tetrazol-2-ol	9283	[30]
13	(H4TTP) Tetra(1H-tetrazol-5-yl)pyrazine	8655	[31]
14	(TNP) N6-(4-nitrobenzyl)-N2-(3-(trifluoromethyl)benzyl)- 9H-purine-2,6-diamine	6876	[32]
15	(TETRYL) Trinitrophenylmethylnitramine	7570	[33]

16	(PETNC) Pentaerythritol tetranitrocarbamate	7686	[34]
17	(CH_3NO_3) Methylnitrate	6300	[35]
18	(MHN) Mannitol hexanitrate	8260	[36]
19	(EGDN) Ethylene glycol dinitrate	7300	[37]
20	(HNS) Hexanitrostilbene1,3,5-Trinitro-2-[2-(2,4,6-trinitrophenyl)ethenyl]benzene	7000	[38]
21	(DNBT) amino-3,5-dinitro-4- pyrazole	8626	[39]
22	(aTRz) Azo-bis-1,2,4-triazole	7800	[40]
23	(CL-20) Hexanitrohexaazaisowurtzitane	9380	[41]
24	DAAT	8800	[42]
25	(H_2BT) 1H,1'H-5,5'-bitetrazole	8109	[43]
26	N-(3,4-dinitro-1H-pyrazol-5-yl)nitramide	9430	[44]
27	(ONC) Octanitrocubane	10100	[45]

Table 5. The descriptors used to build the empirical model.

NO	**Explosive**	**Explosive Velocity**	**E_{HOMO}**	**E_{LUMO}**	**$E_{LUMO-HOMO}$**	**Molecular refractivity**	**Element count**	**Nitro count**
1	HMX	9320	-0.2637	-0.1431	0.12064	58.5691910	4	4
2	3at	8746	-0.2482	-0.1649	0.08329	50.6015930	4	1
3	RDX	8795	-0.2690	-0.1229	0.14606	43.9268950	3	3
4	Picric acid	7376	-0.2700	-0.1825	0.08749	49.7262000	6	3
5	3,4Di (nitramino)furazan	8015	-0.2894	-0.1398	0.14961	38.3049960	2	2
6	FOX-7	8870	-0.2295	-0.1243	0.10518	28.6261960	2	2
7	TNT	6959	-0.2743	-0.1697	0.10459	53.0733070	7	3

8	PETN	8564	-0.2910	-0.1329	0.15811	58.5037160	5	4
9	TATB	8114	-0.2465	-0.1413	0.10519	62.1332930	6	3
10	TMETN	7050	-0.2772	-0.1208	0.15637	50.0350150	5	3
11	ETN	9849	-0.2710	-0.1478	0.12315	53.2546080	4	4
12	5-nitro-2H-tetrazol-2-ol	9283	-0.2725	-0.1573	0.11517	28.5506990	1	1
13	H4TTP	8655	-0.2639	-0.1798	0.08406	100.558594	8	0
14	TNP	6876	-0.1864	-0.1302	0.05625	116.173874	20	1
15	TETRYL	7570	-0.2208	-0.1994	0.02136	63.5535090	7	4
16	PETNC	7686	-0.2552	-0.1587	0.09646	91.4741060	9	4
17	Methyl nitrate	6300	-0.2648	-0.1059	0.15885	14.9552990	1	1
18	MHN	8260	-0.2840	-0.1534	0.13065	78.5675810	6	6
19	EGDN	7300	-0.2883	-0.1243	0.15751	27.9415990	2	2
20	HNS	7000	-0.2696	-0.1795	0.09003	105.460999	14	6
21	DNBT	8626	-0.2471	-0.1511	0.09599	38.7874950	3	2
22	aTRz	7800	-0.1816	-0.1198	0.06178	45.4370000	4	0

23	CL-20	9380	-0.30499	-0.2617	0.04323	81.5153960	6	6
24	DAAT	8800	-0.18200	-0.1448	0.03725	64.2997970	4	0
25	H2BT	8109	-0.2757	-0.1604	0.11522	131.356	2	0
26	N-(3,4-dinitro-1H-pyrazol-5-yl)nitramide	9430	-0.27500	-0.1707	0.10433	182.698	3	3
27	Octanitrocubane	10100	-0.3238	-0.2102	0.11357	355.848	8	8

One empirical equation was built in this study that depends on some structural and electronic descriptors which are HOMO energy (EHOMO), LUMO energy (ELUMO), LUMO-HOMO gap energy (ELUMO-HOMO), Dipole Moment, AlogP, Molecular refractivity, Element count (the number of elements kind in the molecule), Nitro Fragment Count (the number of nitro groups in the molecule), the C-N bond length (AC-N), the electronic density at C-C bond critical point (ρBCPC-C), the electronic density at N-O bond critical point (ρBCPN-O) and the electronic density at the ring critical point (ρRCP). The last three descriptors belong to atom-in-molecules calculations which calculate the charge density at the bonds and the ring of the molecule respectively. The Genetic Function Approximation (GFA) method was used to build the mathematical model. The modeled equation for the calculation of the detonation velocity that is built from those descriptors is the following

Table 5. Continued.

NO	**Explosive**	**$A_{(C-N)}$**	**Dipole Moment**	**ρBCP(N-O)**	**ρBCP (C-C)**	**ρ(RCP**	**AlogP**
1	HMX	1.45685	7.67552	0.442266	---	0.01265	1.503
2	3at	1.41954	9.100575	0.478752	0.283847	0.01896	1.643
3	RDX	1.45505	8.448300	0.450717	---	0.02100	1.128
4	Picric acid	1.44061	2.231062	0.442983	0.308655	0.01987	1.623
5	3,4-Di (nitramino)furazan	---	1.136716	0.455124	0.236505	0.00826	0.419
6	FOX-7	1.40905	9.721301	0.464309	0.280766	0.01593	0.343
7	TNT	1.44468	1.849513	0.456115	0.303901	0.02075	2.375
8	PETN	---	0.001300	0.460132	0.232348	---	1.867
9	TATB	1.41692	0.001792	0.438529	0.274850	0.01569	0.442

10	TMETN	---	7.208 423	0.4562 00	0.2307 98	0.00 911	2.0 14
11	ETN	1.38 422	3.741 347	0.4533 44	0.2742 90	0.05 260	1.9 67
12	5-nitro-2H-tetrazol-2-ol	1.42 271	5.588 600	0.4560 06	---	0.05 949	0.5 08
13	H4TTP	1.32 432	7.000 0e-	---	0.2937 86	0.02 661	0.9 25
14	TNP	1.44 938	8.015 613	0.4528 05	0.2972 60	0.02 566	4.7 71
15	TETRYL	1.43 445	6.782 741	0.4573 33	0.3070 82	0.02 058	1.7 29
16	PETNC	1.36 877	12.18 025	0.4503 88	0.2293 64	0.01 221	0.7 74
17	Methyl nitrate	---	4.424 851	0.4567 53	---	---	0.5 90
18	MHN	---	4.825 972	0.4594 57	0.2394 15	0.01 167	2.9 32
19	EGDN	---	0.001 200	0.4580 88	0.2443 01	---	1.0 02
20	HNS	1.44 756	0.006 438	0.4569 37	0.2447 81	0.02 083	3.9 85
21	DNBT	1.41 031	1.119 522	0.4427 22	0.2790 66	0.05 049	0.6 67
22	aTRz	1.39 807	0.395 200	---	---	0.05 656	1.6 02
23	CL-20	1.46 049	1.888 400	0.4634 81	0.3374 79	0.03 602	1.5 43
24	DAAT	1.40 408	0.042 8	---	---	0.02 786	0.4 11
25	H2BT	1.45 339	0.004 201	---	0.2739 19	0.04 848	0.1 46
26	N-(3,4-dinitro-1H-pyrazol-5-yl)nitramide	1.39 971	4.338 729	0.4893 54	0.2331 47	0.04 372	1.0 25
27	Octanitrocubane	1.45 076	0.001 208	0.4644 50	0.2242 23	0.07 949	1.3 58

Detonation velocity = 71.774 * Molecular refractivity + 3176.962 * ELUMO * Element count + 103.053 * AC-N * Dipole Moment - 3895.921 * ELUMO-HOMO2 * Dipole Moment + 736851.217 * ρRCP2 * ρBCPN-O - 3377.297 * EHOMO * AC-N * ρBCPC-C + 164.769 * ELUMO * Dipole Moment * AlogP - 2000.042 * ELUMO * ρBCPN-O * Nitro Fragment Counts + 5963.317

R^2 = 0.996, Adjusted R^2 = 0.993, Cross validated R^2 = 0.989

The equation is characterized by high R^2, adjusted R^2, and cross-validated R^2 functions with values of 0.996, 0.993, and 0.989 respectively. This makes the model equation robust and has high predictivity for the calculation of the detonation velocity of the explosives. The robustness of the equation is demonstrated by the predicted value of RDX (8794.6 m s-1) which is in excellent agreement with the experimental value of 8795 m s-1 as could be seen in Table 6 which contains the experimental and the predicted detonation velocities as well as the residual values.

From table 6 it is also clear that the predicted detonation velocities by the model equation for other explosives are in good agreement with the experimental values.

Table 6. The experimental predicted, and residual values for the detonation velocities.

No.	Experimental detonation velocity	Predicted detonation velocity	Residuals
1	9320	9351.8	-31.8
2	8746	8763.6	-17.6
3	8795	8794.9	0.1
4	7376	7208.9	167.1
5	8015	7996.0	19.0
6	8870	8886.8	-16.8
7	6959	7086.4	-127.4
8	8564	8539.4	24.6
9	8114	8088.1	25.9
10	7050	7015.1	34.9
11	9849	9797.3	51.7
12	9283	9302.5	-19.5
13	8655	8711.7	-56.7
14	6876	6885.0	-9.0
15	7570	7538.2	31.8
16	7686	7675.7	10.3
17	6300	6316.3	-16.3
18	8260	8297.8	-37.8
19	7300	7407.7	-107.7
20	7000	6997.9	2.1
21	8626	8751.0	-125.0
22	7800	7739.9	60.1
23	9380	9431.5	-51.5
24	8800	8743.6	56.4
25	8109	8071.3	37.7

26	9430	9359.5	70.5
27	10100	10075.1	24.9

4. Conclusion

The electronic energies of the six isomers of the RDX molecule are calculated to be in the sequence twist > AAA> AAE > EEE > EEA > boat indicating that the twist isomer is the most stable. The calculated electronic spectra in acetonitrile showed in most two bands in accordance with the experimental spectrum of RDX. The PBE0/def2-tzvppd// MP2/cc-pVTZ which was used in this study to calculate the spectra was superior to previously used methods and was able to predict fairly the experimental wavelength (236 nm) of the most important band to be 237 nm. The empirical equation modeled in this study shows high robustness represented by R2, adjusted R2 and cross validated R2 with values of 0.996 0993 and 0.989 respectively.

5. References

[1] Q. Wu, W. Zhu, and H. Xiao, "DFT study of structural, electronic, and absorption properties of crystalline β-RDX under pressures," Canadian Journal of Chemistry, vol. 91, no. 10, pp. 968-973, 2013. Doi:https://doi.org/10.1139/cjc-2013-0174

[2] M.-K. Shin, M.-H. Kim, G.-Y. Kim, B. Kang, J.S. Chae, and S. Haam, "Highly Energetic Materials-Hosted 3D Inverse Opal-like Porous Carbon: Stabilization/Desensitization of Explosives," ACS applied materials & interfaces, vol. 10, no. 50, pp. 43857-43864, 2018.Doi:https://doi.org/10.1021/acsami.8b11591

[3] L.E. Dresselhaus-Cooper, D.J. Martynowych, F. Zhang, C. Tsay, J. Ilavsky, S.G. Wang, Y.-S. Chen, and K.A. Nelson, "Pressure-thresholded response in cylindrically shocked cyclotrimethylene trinitramine (RDX)," The Journal of Physical Chemistry A, vol. 124, no. 17, pp. 3301-3313, 2020.Doi:https://doi.org/10.1021/acs.jpca.9b07637

[4] S.K. Singh, V. Vuppuluri, S.F. Son, and R.I. Kaiser, "Investigating the Photochemical Decomposition of Solid 1, 3, 5-Trinitro-1, 3, 5-Triazinane (RDX)," The Journal of Physical Chemistry A, vol. 124, no. 34, pp. 6801-6823, 2020.Doi:https://doi.org/10.1021/acs.jpca.0c05726

[5] Z. Zeng and E.R. Bernstein, "RDX-and HMX-related anionic species explored by photoelectron spectroscopy and density functional theory," The Journal of Physical Chemistry C, vol. 122, no. 39, pp. 22317-22329, 2018.Doi:https://doi.org/10.1021/acs.jpcc.8b07728

[6] Y. Tong, et al., "Exploring the utility of compound-specific isotope analysis for assessing ferrous iron-mediated reduction of RDX in the subsurface," Environmental Science & Technology, vol. 55, no. 10, pp. 6752-6763, 2021.Doi:https://doi.org/10.1021/acs.est.0c08420

[7] M. Guillevic, V. Pichot, J. Cooper, G. Coquerel, L. Borne, and D. Spitzer, "Optimization of an Antisolvent Method for RDX Recrystallization: Influence on Particle Size and Internal Defects," Crystal Growth & Design, vol. 20, no. 1, pp. 130-138, 2020/01/02 2020,Doi:https://doi.org/10.1021/acs.cgd.9b00893.

[8] R.W. Molt, T. Watson, A.P. Bazanté, R.J. Bartlett, and N.G. Richards, "Gas phase RDX decomposition pathways using coupled cluster theory," Physical Chemistry Chemical Physics, vol. 18, no. 37, pp. 26069-26077, 2016.Doi:https://doi.org/10.1039/C6CP05121A

[9] B.A. Saeed, Q.M. Hassan, C. Emshary, H. Sultan, and R.S. Elias, "The nonlinear optical properties of two dihydropyridones derived from curcumin," Spectrochimica Acta Part A: Molecular and Biomolecular Spectroscopy, vol. 240, p. 118622, 2020.Doi:https://doi.org/10.1016/j.saa.2020.118622

[10] L.K. Harper, "Computational investigation of pernicious compounds: Arsenic and high energy density materials and their relevant mechanisms," Old Dominion University, 2015.

[11] C. Devereux et al., "Extending the Applicability of the ANI Deep Learning Molecular Potential to Sulfur and Halogens," Journal of Chemical Theory and Computation, vol. 16, no. 7, pp. 4192-4202, 2020. Doi:https://doi.org/10.1021/acs.jctc.0c00121.

[12] M.e. Frisch, G. Trucks, H.B. Schlegel, G. Scuseria, M. Robb, J. Cheeseman, G. Scalmani, V. Barone, G. Petersson, and H. Nakatsuji, Gaussian 16, Gaussian, Inc. Wallingford, CT, 2016.

[13] A. Barnawi, I. Budhiraja, K. Kumar, N. Kumar, B. Alzahrani, A. Almansour, and A. Noor, "A comprehensive review on landmine detection using deep learning techniques in 5G environment: open issues and challenges," Neural Computing and Applications, vol. 34, no. 24, pp. 21657-21676, 2022.Doi:https://doi.org/10.1007/s00521-022-07819-9

[14] E.A. Musad, R. Mohamed, B.A. Saeed, B.S. Vishwanath, and K.L. Rai, "Synthesis and evaluation of antioxidant and antibacterial activities of new substituted bis (1, 3, 4-oxadiazoles), 3, 5-bis (substituted) pyrazoles and isoxazoles," *Bioorganic & medicinal chemistry letters*, vol. 21, no. 12, pp. 3536-3540, 2011.

[15] A.G. Martynov, J. Mack, A.K. May, T. Nyokong, Y.G. Gorbunova, and A.Y. Tsivadze, "Methodological survey of simplified TD-DFT methods for fast and accurate interpretation of UV–vis–NIR spectra of phthalocyanines," ACS omega, vol. 4, no. 4, pp. 7265-7284, 2019.Doi:https://doi.org/10.1021/acsomega.8b03500.

[16] J. Krupa, M. Wierzejewska, and J. Lundell, "Experimental FTIR-MI and Theoretical Studies of Isocyanic Acid Aggregates," Molecules, vol. 28, no. 3, p. 1430, 2023. Doi:https://doi.org/10.3390/molecules28031430

[17] G.A. Garcia, L. Dontot, M. Rapacioli, F. Spiegelman, P. Bréchignac, L. Nahon, and C. Joblin, "Electronic effects in the dissociative ionisation of pyrene clusters," Physical Chemistry Chemical Physics, vol. 25, no. 6, pp. 4501-4510, 2023.Doi:https://doi.org/10.1039/d2cp05679h

[18] T.G. Mayerhöfer, S. Pahlow, V. Ivanovski, and J. Popp, "Dispersion related coupling effects in IR spectra on the example of water and Amide I bands," Spectrochimica Acta Part A: Molecular and Biomolecular Spectroscopy, vol. 288, p. 122115, 2023. Doi:https://doi.org/10.1016/j.saa.2022.122115

[19] R. Kiralj and M. Ferreira, "Basic validation procedures for regression models in QSAR and QSPR studies: theory and application," Journal of the Brazilian Chemical Society, vol. 20, pp. 770-787, 2009.

[20] G. Wang, Q. Wen, and Y. Wang, "A study of the pore size effect on the formation of hot spot in a 1, 3, 5, 7-tetranitro-1, 3, 5, 7-tetrazocane crystal under a low-to-medium shock velocity," Journal of Energetic Materials, pp. 1-22, 2022.Doi:https://doi.org/10.1080/07370652.2021.2023705

[21] H.-Y. Li, D. Wei, Y.-H. Du, Z.-T. Liu, Z.-X. Bai, F.-S. Liu, and Q.-J. Liu, "Effects of pressure on structural, electronic, optical, and mechanical properties of nitrogen-rich energetic material: 6-azido-8-nitrotetrazolo[1,5-b]pyridazine-7-amine (3at)," Journal of Molecular Modeling, vol. 29, no. 2, p. 43, 2023.Doi:https://doi.org/10.1007/s00894-022-05440-0

[22] B.H. Lee, M.N. Sakano, J.P. Larentzos, J.K. Brennan, and A. Strachan, "A coarse-grain reactive model of RDX: Molecular resolution at the μ m scale," The Journal of Chemical Physics, vol. 158, no. 2, p. 024702, 2023.Doi:https://doi.org/10.1063/5.0122940Art

[23] M. Lv, H. Qian, Z. Dong, and Z. Ye, "Compatibility study of erythritol tetranitrate with some energetic materials," Journal of Thermal Analysis and Calorimetry, vol. 148, no. 3, pp. 711-719, 2023.Doi:https://doi.org/10.1007/s10973-022-11763-0

[24] V.P. Sinditskii, A.A. Kushtaev, N.V. Yudin, A.I. Levshenkov, N.N. Kondakova, and M.A. Alekseeva, "1, 1-Diamino-2, 2-dinitroethylene: The riddles of thermal decomposition and combustion," Journal of Physics and Chemistry of Solids, vol. 177, p. 111275, 2023.Doi:https://doi.org/10.1016/j.jpcs.2023.111275

[25] R.V. Tsyshevsky, S.N. Rashkeev, and M.M. Kuklja, "Control of Explosive Chemical Reactions by Optical Excitations: Defect-Induced Decomposition of Trinitrotoluene at Metal Oxide Surfaces," Molecules, vol. 28, no. 3, p. 953, 2023.Doi:https://doi.org/10.3390/molecules28030953

[26] Y. Zhang, T. Wang, and Y. He, "Initial Response of Pentaerythritol Tetranitrate (PETN) under the Coupling Effect of Preheating, Shock and Defect via the Molecular Dynamics Simulations with the Multiscale Shock Technique Method," Molecules, vol. 28, no. 7, p. 2911, 2023.Doi:https://doi.org/10.3390/molecules28072911

[27] S. Lal, R.J. Staples, and M.S. Jean'ne, "Design and synthesis of phenylene-bridged isoxazole and tetrazole-1-ol based energetic materials of low sensitivity," Dalton Transactions, vol. 52, no. 11, pp. 3449-3457, 2023.Doi:https://doi.org/10.1039/D3DT00166K

[28] W. Pang and L.T. DeLuca, Nano and Micro-Scale Energetic Materials: Propellants and Explosives, John Wiley & Sons, 2023.

[29] D. Hu, Y. Wang, C. Xiao, Y. Hu, Z. Zhou, and Z. Ren, "Studies on ammonium dinitramide and 3, 4-diaminofurazan cocrystal for tuning the hygroscopicity," Chinese Journal of Chemical Engineering, 2023.Doi:https://doi.org/10.1016/j.cjche.2023.01.006

[30] X. Zhang, F. Zou, P. Yang, C. Gao, C. Zhang, M. Zou, X. Cao, W. Hu, and Q. Zhou, "Synthesis and Investigation of 2, 4, 6-Trinitropyridin-3-ol and its Salts," Propellants, Explosives, Pyrotechnics, vol. 45, no. 12, pp. 1853-1858, 2020.Doi:https://doi.org/10.1002/prep.202000177

[31] J. Li, T. Zhou, J. Chen, X. Wang, Y. Wang, W. Liu, X. Zhang, Z. Li, X. Chen, and J. Han, "Theoretical studies on 2, 3, 5, 6-Tetra (1H-tetrazol-5-yl) pyrazine and 1, 1-diamino-2, 2-Dinitroethylene blending system," Journal of Molecular Graphics and Modelling, vol. 116, p. 108235, 2022. Doi:https://doi.org/10.1016/j.jmgm.2022.108235

[32] S. Lee, B.B. Park, H. Kwon, V. Kim, J.S. Jeon, R. Lee, M. Subedi, T. Lim, H. Ha, and D. An, "TNP and its analogs: Modulation of IP6K and CYP3A4 inhibition," Journal of Enzyme Inhibition and Medicinal Chemistry, vol. 37, no. 1, pp. 269-279, 2022.

[33] S.M. ÜNSAL and E. Erkan, "Development and validation of a new RP-HPLC method for organic explosive compounds," Turkish Journal of Chemistry, vol. 46, no. 3, pp. 923-928, 2022.Doi:https://doi.org/10.55730/1300-0527.3380

[34] W. Zhu, "Quantum chemical investigations of reaction mechanism," in Theoretical and Computational Chemistry, Elsevier, pp. 291-345, 2022.Doi:https://doi.org/https://doi.org/10.1016/B978-0-12-822971-2.00004-8

[35] R. Wang and C. Zhang, "Simple Rule for Linking Atoms to Construct High Energy Isomers," Physical Chemistry Chemical Physics, 2023.

[36] Y.-H. Tsai, C.-W. Tsai, and C.A. Tipple, "A validated method for the analysis of sugars and sugar alcohols related to explosives via liquid chromatography mass spectrometry (LC-MS) with post-column addition," Forensic Chemistry, vol. 28, p. 100404, 2022.

[37] A. Simon, T.-H. Ong, A. Wrobel, T. Mendum, and R. Kunz, "Headspace Components of Explosives for Canine Non-Detonable Training Aid Development," Forensic Chemistry, p. 100491, 2023.

[38] P. Gibot, L. Vidal, L. Laffont, and J. Mory, "Zirconia nanopowder synthesis via detonation of trinitrotoluene," Ceramics International, vol. 46, no. 17, pp. 27057-27062, 2020.

[39] X. Han, M. Liu, Z. Huang, H. Huang, X. Long, and B. Tan, "Theoretical Calculation of Cocrystal Components for Explosives: A Similarity Function of Energetic Supramolecules," Crystal Growth & Design, vol. 22, no. 1, pp. 293-303, 2021.Doi:https://doi.org/10.1021/acs.cgd.1c00933

[40] F. Lu, Y. Dong, T. Fei, J. Liu, H. Su, S. Li, and S. Pang, "Noncovalent modification of 4, 4′-azo-1, 2, 4-triazole backbone via cocrystallization with polynitroazoles," Crystal Growth & Design, vol. 19, no. 12, pp. 7206-7216, 2019.Doi:https://doi.org/10.1021/acs.cgd.9b01069

[41] Y. Bayat, G. Taheripouya, V. Zeynali, and V. Azizkhani, "Methods and strategies to achieve hexanitrohexaazaisowurtzitane (HNIW or CL-20): a comprehensive overview," Journal of Energetic Materials, pp. 1-35, 2023.Doi:https://doi.org/10.1080/07370652.2023.2183435

[42] O. T. O'Sullivan and M. J. Zdilla, "Properties and Promise of Catenated Nitrogen Systems As High-Energy-Density Materials," Chemical Reviews, vol. 120, no. 12, pp. 5682-5744, 2020.Doi:https://doi.org/10.1021/acs.chemrev.9b00804.

[43] K.M. Szécsényi and B.B. Holló, "Simultaneous DSC Techniques," in The Handbook of Differential Scanning Calorimetry, Elsevier, pp. 659-791, 2023.Doi:https://doi.org/10.1016/B978-0-12-811347-9.00007-2

[44] J. Das, D. Shem-Tov, S. Zhang, C.-Z. Gao, L. Zhang, C. Yao, E. Flaxer, J. Stierstorfer, M. Wurzenberger, and I. Rahinov, "Power of sulfur–Chemistry, properties, laser ignition and theoretical studies of energetic perchlorate-free 1, 3, 4-thiadiazole nitramines," Chemical Engineering Journal, vol. 443, p. 136246, 2022.Doi:https://doi.org/10.1016/j.cej.2022.136246

[45] Q. Wu, Q. Hu, L. Tan, and W. Zhu, "New cage super insensitive high energy materials constructed by the Diels-Alder reaction based on nitroazoles: A DFT study," Materials Chemistry and Physics, vol. 298, p. 127461, 2023.Doi:https://doi.org/10.1016/j.matchemphys.2023.127461

Journal of Basrah Researches (Sciences) **50**(1), 1 (2024)
DOI: https://doi.org/10.56714/bjrs.50.1.1

دراسة لعلاقة التركيب-الخاصية الكمية لحساب سرعة الانفجار للمتفجرات المشتقة من الار دي اكس مع دراسة اطيافها الالكترونية.

ثائر مجيد حميد، بهجت علي سعيد

قسم الكيمياء، كلية التربية للعلوم الصرفة، جامعة البصرة، البصرة، العراق.

معلومات البحث

الاستلام 9 اذار 2023
القبول 28 اذار 2023
النشر 30 حزيران 2024

الكلمات المفتاحية

متفجر الار دي اكس، علاقة التركيب-الخاصية الكمية، الواصفات، الذرات-في الجزيئات.

الملخص

تركزت الدراسة على تفسير الاطياف الالكترونية لجزيئة الار دي اكس. لقد أجريت خلال الدراسة عمليات الاستمثال الهندسي لايزومرات الار دي اكس الستة أولا باستخدام المستوى النظري MP2/cc-pVTZ. و قد بينت الحسابات ان الايزومر الملتوي هو التركيب الأكثر استقرار من بيت التراكيب الستة. و قد حسبت الاطياف الالكترونية لهذه الايزومرات باستخدام المستوى النظري PBE0/def2-tzvppd في الاسيتوناترايل كمذيب. و قد نجحت الطرق الهجينة PBE0/def2-tzvppd// MP2/cc-pVTZ في تخمين نتائج القياسات التجريبية للحزمة الرئيسية و المقاسة عند 236 نانومتر و بشكل جيد. فقد كانت القيمة المحسوبة 237 نانومتر و بينت الدراسة بانها ناشئة و بشكل رئيسي عن الانتقال هومو – لومو و بأحتمالية مقدارها 0.40688 و التي تمثل نسبة 49.4% من من مجموع الانتقالات المسؤولة عن ظهور هذه الحزمة. و لاجل حساب سرعة الانفجار للمتفجرات المشتقة من الار دي اكس في هذه الدراسة أجريت حسابات التركيب-الخاصية الكمية و تم أنشاء معادلات تجريبية مبنية على سرع الانفجارات المقاسة عمليا لمجموعة من المتفجرات المعروفة إضافة الى مجموعة متنوعة من الواصفات التركيبية و الالكترونية للتراكيب المدروسة.

Citation: T. M. Hamid, B.A. Saeed, J. Basrah Res. (Sci.) **50**(1), 1 (2024). DOI:https://doi.org/10.56714/bjrs.50.1.1

*Corresponding author email: Thiaer270@gmail.com

ISSN: 1817-2695 (Print); 2411-524X (Online)
Online at: https:// jou.jobrs.edu.iq